ACS Photonics

Letter

pubs.acs.org/journal/apchd5

Probing Plasmon-NV^0 Coupling at the Nanometer Scale with Photons and Fast Electrons

Hugo Lourenço-Martins,[†] Mathieu Kociak,[†] Sophie Meuret,[‡] François Treussart,[§] Yih Hong Lee,[∥] Xing Yi Ling,[∥] Huan-Cheng Chang,[⊥] and Luiz Henrique Galvão Tizei*,[†]

[†]Laboratoire de Physique des Solides, Université Paris-Saclay, CNRS UMR 8502, F-91405, Orsay, France
[‡]AMOLF, 1098 XG Amsterdam, Netherlands
[§]Laboratoire Aimé Cotton, CNRS, Université Paris-Sud, ENS Paris-Saclay, Université Paris-Saclay, Orsay 91405, France
[∥]Division of Chemistry and Biological Chemistry, School of Physical and Mathematical Sciences, Nanyang Technological University, Singapore 637371, Singapore
[⊥]Institute of Atomic and Molecular Sciences, Academia Sinica, Taipei 106, Taiwan

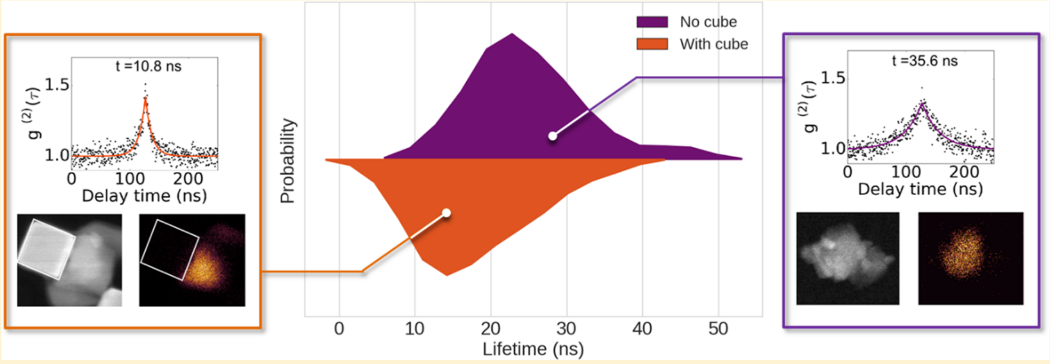

ABSTRACT: The local density of optical states governs an emitters' lifetime and quantum yield through the Purcell effect. It can be modified by a surface plasmon electromagnetic field, but such a field has a spatial extension limited to a few hundreds of nanometers, complicating the use of optical methods to spatially probe emitter−plasmon coupling. Here we show that a combination of electron-based imaging, spectroscopies, and photon-based correlation spectroscopy enables measurement of the Purcell effect with nanometer and nanosecond spatiotemporal resolutions. Due to the large variability of radiative lifetimes of emitters in nanoparticles we relied on a statistical approach to probe the coupling between nitrogen-vacancy centers in nanodiamonds and surface plasmons in silver nanocubes. We quantified the Purcell effect by measuring the nitrogen-vacancy excited state lifetimes in a large number of either isolated nanodiamonds or nanodiamond-nanocube dimers and demonstrated a significant lifetime reduction for dimers.

KEYWORDS: *Purcell effect, lifetime measurement, localized surface plasmon, neutral nitrogen-vacancy defect, electron energy loss spectroscopy, cathodoluminescence*

The radiative lifetime of a light emitter is intrinsically linked to the local density of optical states (LDOS), $\rho(\vec{r}, \omega)$ ($\vec{r}$ represents position in space and ω frequency). The presence of an optical cavity or a plasmonic structure leads to the increase of the LDOS which can be quantified by a transition rate enhancement factor, $\gamma = \rho(\vec{r}, \omega)/\rho_0(\vec{r}, \omega)$[1] ($\rho$ and ρ_0 being the LDOS with and without the a cavity or plasmonic structure), what is known as Purcell effect.[2] Owing to the Fermi golden rule, the radiative lifetime of an emitter interacting with these photonic structures is modified by γ. Due to the short lifetime of surface plasmons (SP)[3] (typically few femtoseconds), their coupling with quantum emitters (QE) is usually weak. In this regime, the Purcell effect is predominant.

To date, only two strategies have been considered to measure the Purcell effect in QE-SP dimers. From a microscopic perspective, experiments were carried out on a single dimer[4−7] with a precise positioning of the QE. Alternatively, macroscopic measurements were performed simultaneously on a large ensemble of dimers.[8,9] Both approaches present limitations due to the large variability of the isolated QEs lifetimes.[10−13]

Here, to overcome this intrinsic variability we adopt a statistical method applied to individual nano-objects, where the lifetime of large sets of isolated QEs and dimers are measured. In our experiments, neutral nitrogen-vacancy (NV^0) centers dipoles in nanodiamonds were coupled to surface plasmons on Ag nanocubes. To quantify the Purcell effect at the nanoscale,

Received: September 19, 2017
Published: November 13, 2017

DOI: 10.1021/acsphotonics.7b01093
ACS Photonics 2018, 5, 324−328

we applied a combination of electron-based imaging, spectroscopies, and photon-based correlation spectroscopy that allowed us to achieve the required spatial and temporal resolutions with large throughput.

Modern scanning transmission electron microscopes (STEM) are versatile, allowing the use of nanometer-wide electron probes to obtain complementary information from spectroscopic, diffraction and imaging techniques. Specifically electron energy loss spectroscopy (EELS) and cathodoluminescence (CL) have shown their remarkable capability to measure absorption and emission spectra with nanometer spatial resolution.[14−17] Figure 1 shows a typical EEL spectrum for an isolated Ag nanocube and a CL spectrum for an isolated nanodiamond containing NV^0 centers. The EEL spectrum presents three peaks corresponding to different plasmon modes. The peak at 1.8 eV with a 500 meV width matches the energy range of the NV^0 emission, indicating the possibility of coupling between SP and the NV^0 centers. We note that SP spatial intensity distribution is highly anisotropic, as seen in Figure 1c,d for the mode at 1.8 eV. In principle, this could play a role into where the nanodiamond should be positioned. As discussed later, this does not play a major role due to the large spatial extent of SP modes.

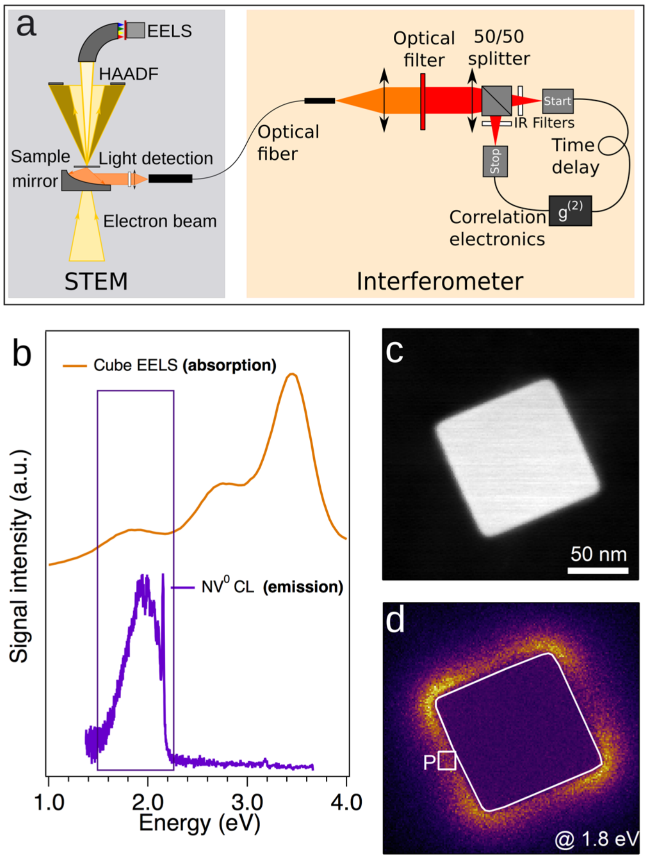

Figure 1. (a) Schematic of the STEM and HBT interferometer setup. (b) EELS spectrum (absorption) of a Ag nanocube measured in region *P* indicated in (d). Each peak corresponds to a plasmon resonance. The purple rectangle indicates the energy window where the optical filter is active. (c) ADF image of a Ag nanocube. (d) Energy filtered (at 1.8 eV) EELS map of the silver nanocube showed in (c).

Lifetimes of isolated nanodiamonds and nanodiamonds/nanocubes dimers have been inferred from the second order correlation function ($g^{(2)}(\tau)$) of light emitted from NV^0 centers excited by the fast electrons, as already demonstrated for different systems.[18−21] In short, each electron excites more than one electron−hole pair above the bandgap of diamond. These pairs excite within a few picoseconds more than one localized defect. The end result is the emission of more than one photon within the emitter's lifetime, leading to the effective formation of a light pulse and a second order correlation function presenting a bunching behavior. This bunching peak has a time decay constant equal to the emitter's total lifetime, allowing its measurement. Note that lifetimes can also be measured using a pulsed electron source and a cathodoluminescence setup, but with limited spatial resolution (50 nm) up to now.[22] $g^{(2)}(\tau)$ was measured using a Hanbury Brown and Twiss (HBT) interferometer (see Figure 1a) coupled to the light collection system.[23] Annular dark field (ADF) images allows us to determine the position of the nanodiamond with respect to the nanocube and the nanocube size with a nanometer resolution, giving us all the parameters necessary to estimate the expected enhancement factor.

Samples were prepared by sequentially drop casting solutions of Ag nanocubes and nanodiamonds containing multiple NV^0 centers onto a 15 nm thick Si_3N_4 membrane. Nanodiamonds typically appear as aggregates (Figure 1a). However, among these aggregates a larger and luminescent nanoparticle is always observed, which is the one considered in each measurement. Most of the nanodiamonds tend to be adsorbed on the nanocubes faces. Moreover, a distribution of sizes is observed in our nanocubes sample (100 nm average size with some variation). This influences the energy of a specific SP. But as a continuum of SP modes is observed for every given nanocube and the NV^0 emission is spectrally wide, coupling is always possible. Isolated nanodiamonds and dimers were identified using ADF images that are acquired simultaneously with wavelength filtered CL maps (first and second columns in Figure 2). Quick access to this information allows an effortless identification. After a target isolated nanodiamond or dimer is selected, the $g^{(2)}(\tau)$ function of the emitted photons is measured using the HBT interferometer while the electron beam scans a fixed small area on the nanodiamond. The photon counting rate and the ADF image can be recorded live, allowing sample drift to be corrected by repositioning the scanning area. In total, the lifetime of 56 isolated nanodiamonds and 62 dimers were measured in the same sample in a single experimental run, ensuring identical experimental conditions.

Examples of measurements in two isolated nanodiamonds and two dimers are shown in Figure 2a,b and c,d, respectively. The isolated nanodiamond in Figure 2a and the dimer in Figure 2d have lifetimes 36 ± 5 ns and $\tau = 11 \pm 1$ ns, respectively, in agreement with an enhancement effect. However, isolated nanodiamonds and dimers (Figure 2b,c) with similar lifetimes are also present ($\tau = 22 \pm 2$ ns and $\tau = 21 \pm 1$ ns in these examples). Such observations occur due to the large dispersion in NV^0 lifetimes in nanodiamonds already reported in the literature.[11,24,25] The lifetime for NV^0 in bulk diamond is 19 ns[26] and it is distributed between 10 and 40 ns[11] in nanodiamond. A similar behavior is known for the NV^- (charged NV) center, for which the lifetime changes from 13 ns in bulk[27] to larger values (17 and 25 ns) in nanoparticles,[24,25] with a broad distribution.[28] The excited state lifetime increase is the result of the smaller LDOS in nanoparticle than in bulk (i.e., $\gamma < 1$, as predicted in the electrostatic regime of particle size smaller than the vacuum

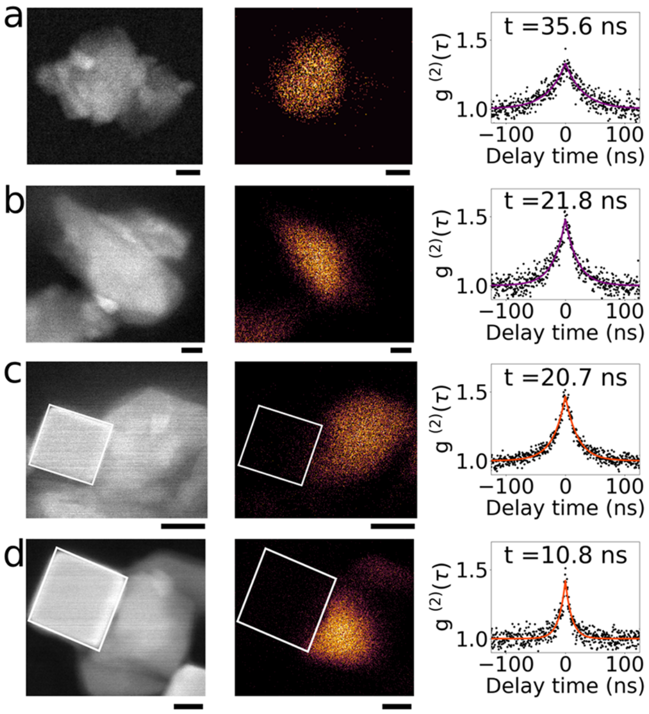

Figure 2. (a, b) From left to right: ADF image, energy-filtered NV^0 emission intensity image and $g^{(2)}$ correlation function of single nanodiamonds. (c, d) From left to right: ADF image, energy filtered CL maps (see Figure 1), and $g^{(2)}$ correlation function of nanodiamonds close to a silver nanocube. Scale bars: 50 nm.

emission wavelength of the embedded emitter), while the lifetime dispersion is mainly due to nanoparticle size variability.[29]

To overcome this variability, a measurement of the Purcell effect can be performed by sequentially probing the NV^0 lifetime of an isolated nanodiamond, followed by coupling the nanodiamond to a plasmonic structure (either by mechanical movement or lithography), as shown by Beams et al.[7] However, this approach would normally involves taking the sample out of vacuum and performing a series of processes which can modify its local environment and, hence, its lifetime. Here we overcome the variability by measuring the excited state lifetime in a large ensemble of either isolated nanodiamonds or dimers.

The histograms (top) and a scattered plot (bottom) of the lifetime of isolated nanodiamonds (purple) and dimers (orange) are shown in Figure 3 (see SI for the complete data set). The average lifetimes of isolated nanodiamonds and dimers are 24 ± 5 ns and 18 ± 4 ns (the most probable values are 22.5 ± 2.5 ns and 12.5 ± 2.5 ns). The two distributions overlap. However, they are significantly distinct, as confirmed by the Wilcoxon−Mann−Whitney statistical u-test ($p = 1.91 \times 10^{-6}$). Therefore, the 40% reduction of lifetimes can be unambiguously associated with a Purcell effect with a spontaneous decay rate enhancement factor of 1.4, indicating some coupling, although weak, between NV^0 centers in nanodiamonds and SP in Ag nanocubes.

Lifetimes shorter than that in bulk are observed in both histograms of Figure 3, although with a small probability. These occur due to nonradiative decay channels involving, for example, surface defects, which do affect the excited state lifetime. Overall, the coupling leads to a rigid shift of NV^0 lifetime histogram to shorter values. These features are only accessible with a statistical approach which emphasizes the strength of our experimental method.

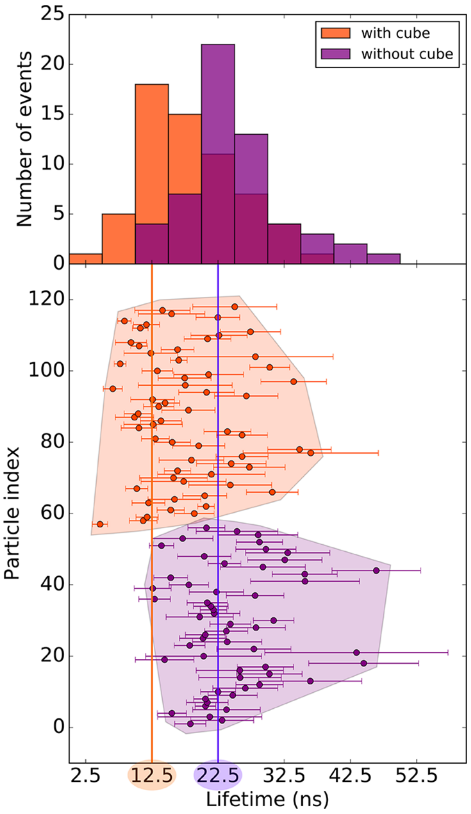

Figure 3. Distribution of nanodiamonds cathodoluminescence lifetime alone (purple) and close to a silver nanocube (orange) measured on a population of 118 diamonds. The two vertical lines indicate the maxima of the nanodiamonds' lifetime distribution alone (22.5 ± 2.5 ns in purple) and close to a silver nanocube (12.5 ± 2.5 ns in orange).

As recently pointed out,[30] the calculation of the luminescence enhancement of defects in the presence of a plasmonic field is an intricate problem. A quantitative simulation of our experiment would require precise knowledge of a large set of parameters: the shape of the nanodiamonds, exact number of defects, their position in the nanoparticle, their respective lifetime, and the profile of the plasmonic field within the nanodiamond. Although we do not tackle this problem in the current paper, we have performed numerical calculations to verify that the order of magnitude of the expected effect matches our observations. A key point for these calculations is the presence of numerous NV^0s in our nanodiamonds. In principle, the NV^0 lifetime may vary with the position of the emitter within a nanoparticle for subwavelength-sized nanodiamonds (electrostatic regime) but experimentlly we have observed that it is constant throughout the nanodiamond, as pointed out by Greffet et al.[29] No variations within the same nanodiamond was observed, despite the nanometer spatial resolution provided by our experiments. Even if electron−hole diffusion in the nanodiamond could decrease our expected spatial resolution (as it is known to occur[31]), variations of NV^0s lifetime could be observed if they occurred at scales larger than 50 nm.

The expected radiative rate enhancement factor due to the Purcell effect was calculated by considering an isolated Ag nanocube, taken the Si_3N_4 substrate into account. Calculations performed with the MNPBEM toolbox[32] show a SP mode centered at 2.1 eV, in agreement with the experimental value (Figure 1a). Considering that most nanodiamonds were observed on a facet of the nanocubes, we calculated the LDOS enhancement factor at 2.1 eV along a line centered on a nanocube face and perpendicular to it, for an emitter at a distances between 10 and 100 nm from the nanocube surface (arrow on Figure 4).

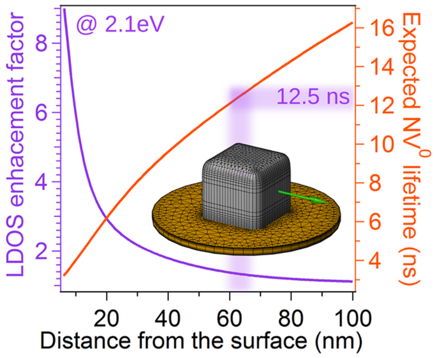

Figure 4. (Purple) LDOS enhancement factor, γ due to SP sustained by an Ag cube, at 2.1 eV calculated along the green arrow represented on the inset. (Orange) Corresponding expected NV^0 lifetime. When the LDOS enhancement factor is equal to one, the lifetime is assumed to be 22.5 ns (as measured in Figure 3).

The enhancement factor is plotted on Figure 4 (purple). Taking into account that the most probable lifetime for NV^0 in isolated nanodiamonds is 22.5 ns, we plotted in orange the expected NV^0 lifetime given the calculated enhancement factor. We see that the most probable lifetime measured in the presence of a nanocube (12.5 ns) corresponds to a distance of 65 nm, also associated with the enhancement factor 1.4. This value is in qualitative agreement with the possible distance of a NV^0 center to the surface of a 100−200 nm nanodiamond (sizes typically observed in our sample). Although this result relies on the specific positioning of the emitters in the dimer, obtaining a consistent distance value is a strong evidence to support our conclusion.

We have used a combination of fast electron/photon techniques to quantify the Purcell effect resulting from the coupling of dipolar emitters embedded in nanoparticles to plasmonic structures. NV^0 in nanodiamond-SP coupling is evidenced by the reduction of the mean excited state lifetime going from individual isolated nanodiamonds to dimers. This effect could have been masked if we had limited our study to a few objects because of the instrinsic lifetime dispersion. We have shown that the combination of fast electron/photon techniques provides the required measurement throughput, spatial and temporal resolutions to disentangle the two effects. The ensemble of techniques described here can be applied seamlessly to any emitter with excited state lifetime in the 0.5−50 ns range, which emit light under electron irradiation, covering a wide range of nanoscale systems.

■ METHODS

Experiments have been performed with a Vacuum Generator HB-501 STEM equipped with a cold field emission electron gun operating at 60 kV, a home-made EEL spectrometer and the Attolight Mönch 4107 Cl-system. An homemade HBT interferometer has been implemented on the nano-CL system (Figure 1a). The stage of the microscope is cooled with liquid nitrogen down to 150 K. EEL spectrum images were deconvolved using a Richardson-Lucy algorithm,[33] with a zero-loss peak (ZLP) width reduction from 0.33 to 0.1 eV. Lifetimes were measured as described by Meuret et al.,[18,19] allowing measurements in a few tens of seconds. The $g^{(2)}(\tau)$ measurements were performed with sampling time of 512 ps, using τ-SPADs single photon avalanche photodiodes and a PicoHarp 300 from PicoQuant. The overall system has a response time of 130 ps. Nanocubes were synthesized via a polyol reduction route.[34]

■ AUTHOR INFORMATION

Corresponding Author

*E-mail: luiz.galvao-tizei@u-psud.fr.

ORCID

Mathieu Kociak: 0000-0001-8858-0449
Yih Hong Lee: 0000-0003-1869-5835
Xing Yi Ling: 0000-0001-5495-6428
Huan-Cheng Chang: 0000-0002-3515-4128
Luiz Henrique Galvão Tizei: 0000-0003-3998-9912

Notes

The authors declare no competing financial interest.

■ ACKNOWLEDGMENTS

This work was financially supported by the National Agency for Research under the program of future investment TEMPOS-CHROMATEM with the reference ANR-10-EQPX-50.

■ REFERENCES

(1) Novotny, L.; Hecht, B. *Principles of Nano-Optics*; Cambridge University Press: Cambridge, 2006; p 578.

(2) Purcell, E. M.; Torrey, H. C.; Pound, R. V. Resonance Absorption by Nuclear Magnetic Moments in a Solid. *Phys. Rev.* **1946**, *69*, 37−38.

(3) Bosman, M.; Ye, E.; Tan, S. F.; Nijhuis, C. A.; Yang, J. K. W.; Marty, R.; Mlayah, A.; Arbouet, A.; Girard, C.; Han, M.-Y. Surface plasmon damping quantified with an electron nanoprobe. *Sci. Rep.* **2013**, *3*, 1312.

(4) Farahani, J. N.; Pohl, D. W.; Eisler, H. J.; Hecht, B. Single quantum dot coupled to a scanning optical antenna: A tunable superemitter. *Phys. Rev. Lett.* **2005**, *95*, 1−4.

(5) Kuhn, S.; Hakanson, U.; Rogobete, L.; Sandoghdar, V. Enhancement of single-molecule fluorescence using a gold nanoparticle as an optical nanoantenna. *Phys. Rev. Lett.* **2006**, *97*, 1−4.

(6) Schietinger, S.; Barth, M.; Aichele, T.; Benson, O. Plasmon-enhanced single photon emission from a nanoassembled metal - Diamond hybrid structure at room temperature. *Nano Lett.* **2009**, *9*, 1694−1698.

(7) Beams, R.; Smith, D.; Johnson, T. W.; Oh, S. H.; Novotny, L.; Vamivakas, A. N. Nanoscale fluorescence lifetime imaging of an optical antenna with a single diamond NV center. *Nano Lett.* **2013**, *13*, 3807−3811.

(8) Aberra Guebrou, S.; Symonds, C.; Homeyer, E.; Plenet, J. C.; Gartstein, Y. N.; Agranovich, V. M.; Bellessa, J. Coherent Emission from a Disordered Organic Semiconductor Induced by Strong Coupling with Surface Plasmons. *Phys. Rev. Lett.* **2012**, *108*, 066401.

(9) Fedutik, Y.; Temnov, V. V.; Schöps, O.; Woggon, U.; Artemyev, M. V. Exciton-plasmon-photon conversion in plasmonic nanostructures. *Phys. Rev. Lett.* **2007**, *99*, 1−4.

(10) Fisher, B.; Eisler, H. Emission intensity dependence and single-exponential behavior in single colloidal quantum dot fluorescence lifetimes. *J. Phys. Chem. B* **2004**, *108*, 143−148.

(11) Storteboom, J.; Dolan, P.; Castelletto, S.; Li, X.; Gu, M. Lifetime investigation of single nitrogen vacancy centres in nanodiamonds. *Opt. Express* **2015**, *23*, 11327−11333.

(12) Lim, T.-S.; Fu, C.-C.; Lee, K.-C.; Lee, H.-Y.; Chen, K.; Cheng, W.-F.; Pai, W. W.; Chang, H.-C.; Fann, W. Fluorescence enhancement and lifetime modification of single nanodiamonds near a nanocrystalline silver surface. *Phys. Chem. Chem. Phys.* **2009**, *11*, 1508.

(13) Andersen, S. K. H.; Kumar, S.; Bozhevolnyi, S. I. Coupling of nitrogen-vacancy centers in a nanodiamond to a silver nanocube. *Opt. Mater. Express* **2016**, *6*, 916−922.

(14) Nelayah, J.; Kociak, M.; Stéphan, O.; García de Abajo, F. J.; Tencé, M.; Henrard, L.; Taverna, D.; Pastoriza-Santos, I.; Liz-Marzán, L. M.; Colliex, C. Mapping surface plasmons on a single metallic nanoparticle. *Nat. Phys.* **2007**, *3*, 348−353.

(15) Zagonel, L. F.; Mazzucco, S.; Tenc, M.; March, K.; Bernard, R.; Tchernycheva, M.; Rigutti, L.; Julien, F. H.; Songmuang, R.; Kociak, M. Nanometer scale spectral imaging of quantum emitters in nanowires and its correlation to their atomically resolved structure. *Nano Lett.* **2011**, *11*, 568−573.

(16) Losquin, A.; Zagonel, L. F.; Myroshnychenko, V.; Rodríguez-González, B.; Tencé, M.; Scarabelli, L.; Förstner, J.; Liz-Marzán, L. M.; García De Abajo, F. J.; Stéphan, O.; Kociak, M. Unveiling nanometer scale extinction and scattering phenomena through combined electron energy loss spectroscopy and cathodoluminescence measurements. *Nano Lett.* **2015**, *15*, 1229−1237.

(17) Kociak, M.; Zagonel, L. Cathodoluminescence in the scanning transmission electron microscope. *Ultramicroscopy* **2017**, *174*, 50−69.

(18) Meuret, S.; Tizei, L. H. G.; Cazimajou, T.; Bourrellier, R.; Chang, H. C.; Treussart, F.; Kociak, M. Photon bunching in cathodoluminescence. *Phys. Rev. Lett.* **2015**, *114*, 1−5.

(19) Meuret, S.; Tizei, L. H. G.; Auzelle, T.; Songmuang, R.; Daudin, B.; Gayral, B.; Kociak, M. Lifetime Measurements Well below the Optical Diffraction Limit. *ACS Photonics* **2016**, *3*, 1157−1163.

(20) Meuret, S.; Coenen, T.; Zeijlemaker, H.; Latzel, M.; Christiansen, S.; Conesa-Boj, S.; Polman, A. Photon bunching reveals single-electron cathodoluminescence excitation efficiency in InGaN quantum wells. *Phys. Rev. B: Condens. Matter Mater. Phys.* **2017**, *96*, 035308.

(21) Tizei, L. H. G.; Kociak, M. Chapter Four-Quantum Nanooptics in the Electron Microscope. *Adv. Imaging Electron Phys.* **2017**, *199*, 185−235.

(22) Merano, M.; Sonderegger, S.; Crottini, A.; Collin, S.; Renucci, P.; Pelucchi, E.; Malko, A.; Baier, M. H.; Kapon, E.; Deveaud, B.; Ganière, J.-D. Probing carrier dynamics in nanostructures by picosecond cathodoluminescence. *Nature* **2005**, *438*, 479−82.

(23) Tizei, L. H. G.; Kociak, M. Spatially resolved quantum nano-optics of single photons using an electron microscope. *Phys. Rev. Lett.* **2013**, *110*, 1−5.

(24) Tisler, J.; et al. Fluorescence and Spin Properties of Defects in Single Digit Nanodiamonds. *ACS Nano* **2009**, *3*, 1959−1965.

(25) Beveratos, A.; Brouri, R.; Gacoin, T.; Poizat, J.-P.; Grangier, P. Nonclassical radiation from diamond nanocrystals. *Phys. Rev. A: At., Mol., Opt. Phys.* **2001**, *64*, 61802.

(26) Liaugaudas, G.; Davies, G.; Suhling, K.; Khan, R. U. A.; Evans, D. J. F. Luminescence lifetimes of neutral nitrogen-vacancy centres in synthetic diamond containing nitrogen. *J. Phys.: Condens. Matter* **2012**, *24*, 435503.

(27) Collins, A. T.; Thomaz, M. F.; Jorge, M. I. B. Luminescence decay time of the 1.945 eV centre in type Ib diamond. *J. Phys. C: Solid State Phys.* **1983**, *16*, 2177−2181.

(28) Inam, F. A.; Gaebel, T.; Bradac, C.; Stewart, L.; Withford, M. J.; Dawes, J. M.; Rabeau, J. R.; Steel, M. J. Modification of spontaneous emission from nanodiamond colour centres on a structured surface. *New J. Phys.* **2011**, *13*, 073012.

(29) Greffet, J. J.; Hugonin, J. P.; Besbes, M.; Lai, N. D.; Treussart, F.; Roch, J. F. Diamond particles as nanoantennas for nitrogen-vacancy color centers. *arXiv:1107.0502* **2011**, na.

(30) Meng, X.; Liu, S.; Dadap, J. I.; Osgood, R. M. Plasmonic enhancement of a silicon-vacancy center in a nanodiamond crystal. *Physical Review Materials* **2017**, *1*, 015202.

(31) Tizei, L. H. G.; Kociak, M. Spectrally and spatially resolved cathodoluminescence of nanodiamonds: local variations of the NV^0 emission properties. *Nanotechnology* **2012**, *23*, 175702.

(32) Hohenester, U.; Trügler, A. A Matlab toolbox for the simulation of plasmonic nanoparticles. *Comput. Phys. Commun.* **2012**, *183*, 370−381.

(33) Gloter, A.; Douiri, A.; Tence, M.; Christian, C. Improving energy resolution of EELS spectra: an alternative to the monochromator solution. *Ultramicroscopy* **2003**, *96*, 385−400.

(34) Tao, A.; Sinsermsuksakul, P.; Yang, P. Polyhedral silver nanocrystals with distinct scattering signatures. *Angew. Chem., Int. Ed.* **2006**, *45*, 4597−4601.